Physical and sensing characterization of nanostructured Ag doped TiO_2 thin films

M. S. Sada [a], R. I. Jasim[b], A. M. Saleh[a,*], K. N. Hussein[d], N. F. Habubi[e], S. S. Chiad[b]

[a]*Department of Physics, College of Education, University of Masan, Iraq*
[b]*Department of Physics, College of Scienc, Mustansiriyah University, Iraq*
[c] *Department of Physics, College of Education, University of Garmian, Iraq*
[d]*Department of Radiology, Al-Manara College for Medical Science, Iraq*
[e]*Department of Radiation and Sonar Technologies, Alnukhba, University College, Iraq*

On glass substrates, silver (Ag) doped Titanium dioxide (TiO_2) films at varied levels of concentrations (0, 2, and 4) % wt were synthesized by chemical spray pyrolysis (CSP). As per the X-ray diffraction pattern, the only phases present in the sample were anatase and rutile TiO_2. Using AFM, it was discovered that the TiO_2 thin films were smooth and compact; however, the surface roughness increases as the dopant amount decreases. SEM images display TiO_2 films. Surface transformation is evident with uniform spherical nano-grains after Ag doping. The optical characteristics of wavelength range (300-900) nm have been investigated using absorbance and transmittance spectra. The results revealed that the films have a 65-75 % transmittance in VIS-NIR spectra for all films. The allowable direct electronic transitions have (3.15-3.25) eV energy gaps. At 250 ppm, the NH_3 gas sensor exhibited increased resistance, indicating heightened sensitivity. Sensitivity decreases with concentration increases to 0 %, 2 %, and 4 % of Ag for NH_3 gas. Reduction observed: 18.4% to 4.6% (50 ppm), 20.7% to 6.8% (150 ppm), and 25.9% to 8.2% (250 ppm).

(Received January 11, 2024; Accepted April 15, 2024)

Keywords: TiO_2, Ag content, Optical and structural properties, Atomic force microscope, SEM, Energy gap, Gas senor

1. Introduction

TiO_2 has been extensively researched and applied in diverse sectors such as electrical, chemical, architectural, pharmaceutical, and cosmetic industries for over two decades. Its popularity in scientific investigations stems from its exceptional catalytic properties, cost-effectiveness, robust physical and chemical stability, and non-toxic composition [1]. TiO_2 exists in three polymorphic forms: brookite, anatase, and rutile, with the latter two commonly utilized as photocatalysts. Anatase and brookite, as metastable phases, undergo transformation to rutile within the temperature range of 973 K to 1173 K.. Anatase and rutile have a tetragonal structure, while brookite has an orthorhombic structure [2]. The photocatalytic activity of TiO_2 is widely understood to be linked to its crystal structure. [3]. Dopants are picked based on a range of features like the number of doped atom size contrast to the host atom and whether they are cationic or anionic. All of these variables impact several properties, including morphological, optical, and electrical characteristics[4]. Several publications have been published in this metal oxide [5–7]. The ionic radii of Ag^+ ion (1.15Å) are bigger than that of Ti^{4+} ion (0.68Å)), the Ag^+ ions [8-9]. The introduction of Ag onto pristine TiO_2 significantly alters the electrical and optical properties of semiconducting materials through impurity doping. [10]. TiO_2 is grown using a variety of processes, such as, CVD [11], ion beam [112], PECVD [13], Plasma spray [14],anodic [15], PLD [16], including thermal [17], sol–gel method [18-20], RF sputtering method [20, 21] and CSP [22-

* Corresponding author: adnan.mahmud@garmian.edu.krd
https://doi.org/10.15251/JOR.2024.202.255

25]. The major goal of this research was to use the CSP method to produce undoped and TiO_2:Ag thin films and explore the doping influence on several physical parameters.

2. Experimental

The TiO_2 thin films were made by dissolving 0.1 M $TiCl_2$ (provided by Sigma-Aldrich – Germany) in a 1:1 deionized water and ethanol solution. Ag trichloride ($AgCl_3$), diluted in deionized water (supplied by PubChem India), was used as a doping agent. The insertion of a few drops of HCl resulted in a transparent solution. Ag-doped TiO_2 film was grown on a glass slide base by chemical spray pyrolysis. The conditions for preparation are as follows: Substrate temperature 450°C, The distance between the spout and base was 29 cm, and 8 S spraying time was extended to 60 seconds to prevent cooling, with a spray rate of 4 ml/min, and nitrogen (N_2) was utilized as a carrier gas.. Film thickness was determined to be 330 ±25 nm using the gravimetric technique. XRD obtained the structural properties. AFM was utilized to study surface of the deposited films. SEM was employed for morphology analysis. UV-visible spectrophotometer was utilized to record absorbance spectra in the 300-900 nm wavelength region. In conclusion, The TiO_2 gas sensor was fabricated by depositing aluminum as ohmic contact electrodes on the TiO_2 thin films using a graded mask. Gas sensitivity is typically assessed by the percentage change in film resistance upon exposure. The samples were placed in a locally manufactured cylindrical chamber (radius: 7.5 cm, height: 15 cm) for testing.

3. Results and discussions

Figure 1 illustrates the XRD patterns of the intended films, revealing the impact of Ag on the phase of TiO_2 films.. The TiO_2 phase shows three dominant peaks at 28.56°, 36.64°, 43.51°, 57.31° and 61.67° attributed to the (002), (202), (003), (022) and (313) planes, respectively. Adding Ag could improve the crystallization of the TiO_2 films. All the films exhibit the phases of anatase and rutile, both belonging to the tetragonal crystal system. The peak is similar to the standard ICDD card No (46-1238). No additional diffraction peaks belonging to silver or silver compounds exist in the diffraction patterns of all the samples, mentioning that metal ions are dispersed on TiO_2 [26]. This can be attributed to the low amount of dopants in these samples or the replacement of Ti ions with Ag ions. Ag doped TiO_2 thin films diffraction peak is slightly shifted upward compared with the undoped TiO_2 thin films. Average crystallite size of TiO_2 Compared with Ag-doped TiO_2 has been increased with doping which slightly increases this attribute to annealing films with preparation. Because of the existence of ionic radii mismatch, the doping of Ag induces a dislocation density and strain in the TiO_2 crystal lattice; Given that Ag^+(1.26) has a higher ionic radius than Ti^{4+}(0.68), a small amount of Ag^+ can be introduced into the periodic crystal lattice of TiO_2 by substituting Ti^{4+} ions, but this is not significant. [27,28].

The formula developed by Debye Scherrer can be written as [29].

$$D_{hkl} = \frac{0.9\lambda}{\beta cos\theta} \tag{1}$$

Here, λ represents the incident X-ray wavelength, β is the Full Width at Half Maximum (FWHM), and θ is the diffraction angle.The lattice dislocation densities formula can be expressed as [30]:

$$\delta = \frac{1}{D^2} \tag{2}$$

The lattice strain formula can be expressed as [31]:

$$\varepsilon = \frac{\beta cos\theta}{4} \tag{3}$$

Table 1 shows the decrease in strain and dislocation density with increased crystallite size, indicating better crystallinity with increased Ag doping. This attributes more defects in the crystal lattice and lattice distortion in Ag-doped TiO_2 films [32].

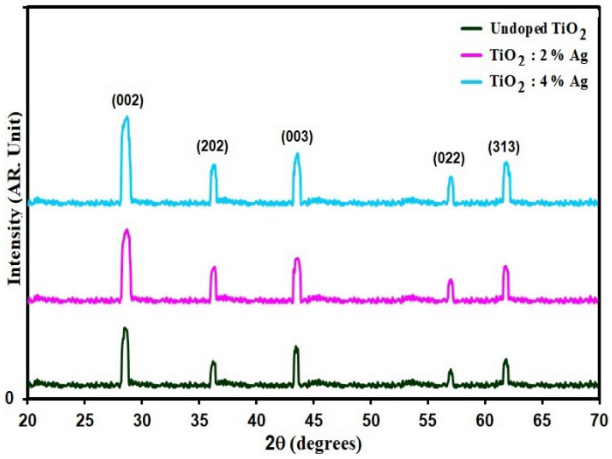

Fig. 1. XRD styles of the intended films.

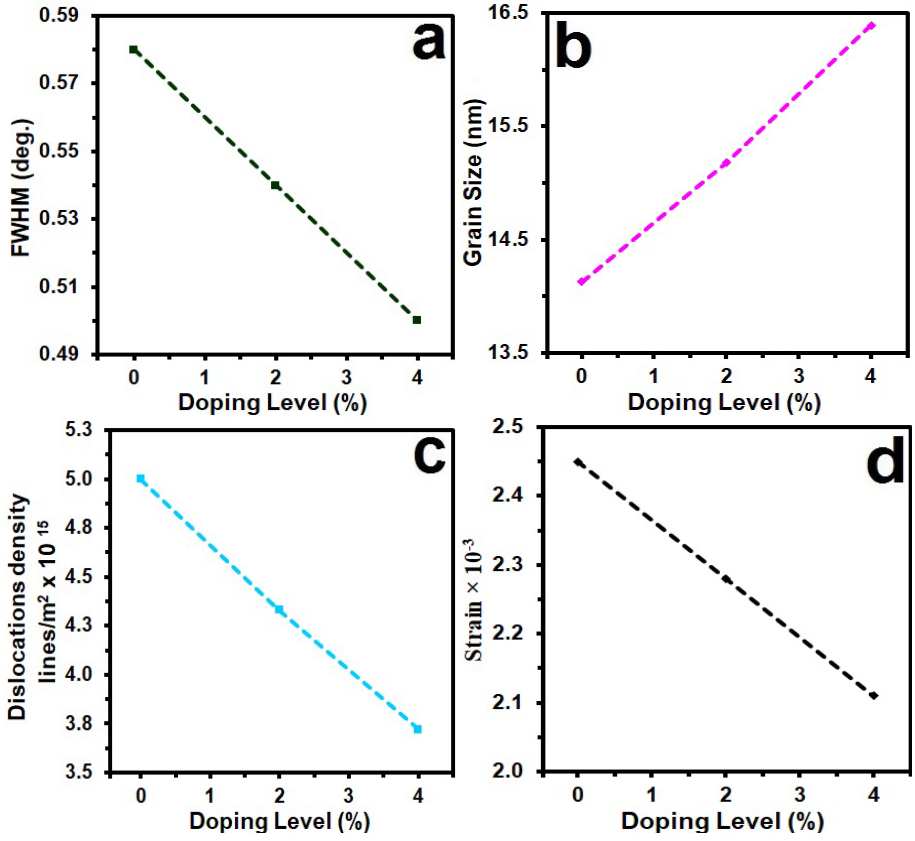

Fig. 2. X-ray parameters of the intended films.

Table 1. Microstructural parameters of the intended films.

Specimen	2 θ (°)	(hkl) Plane	FWHM (°)	Optical bandgap (eV)	Grain size (nm)	Dislocations density ($\times 10^{15}$) (lines/m^2)	Strain ($\times 10^{-3}$)
Undoped TiO_2	28.56	002	0.58	3.25	14.13	5.00	2.45
TiO_2: 2% Ag	28.56	002	0.54	3.20	15.18	4.33	2.28
TiO_2: 4% Ag	28.47	002	0.50	3.15	16.39	3.72	2.11

AFM studies, in general, complement the results obtained from three-dimensional imaging. The undoped and TiO_2: Ag films are uniform, dense, crack-free and homogeneous. In Fig. (3), we give the AFM image of the Undoped and TiO_2: Ag surface. The estimated average particle size measurement of the TiO_2 surface is about 76.82nm and decreases with Ag 3% doping to arrive 55.43 nm. The surface roughness's surface root mean square (RMS) values amounted to 5.86nm and 3.16nm for as-deposited TiO_2 and TiO_2: Ag (3%)films, respectively. Doping TiO_2 with Ag significantly decreased surface smoothness of the film. The average particle size is in the nm range, slightly larger than the XRD data. Similar results can be seen in reference [33]. Table 2 illustrates the AFM information for all films.

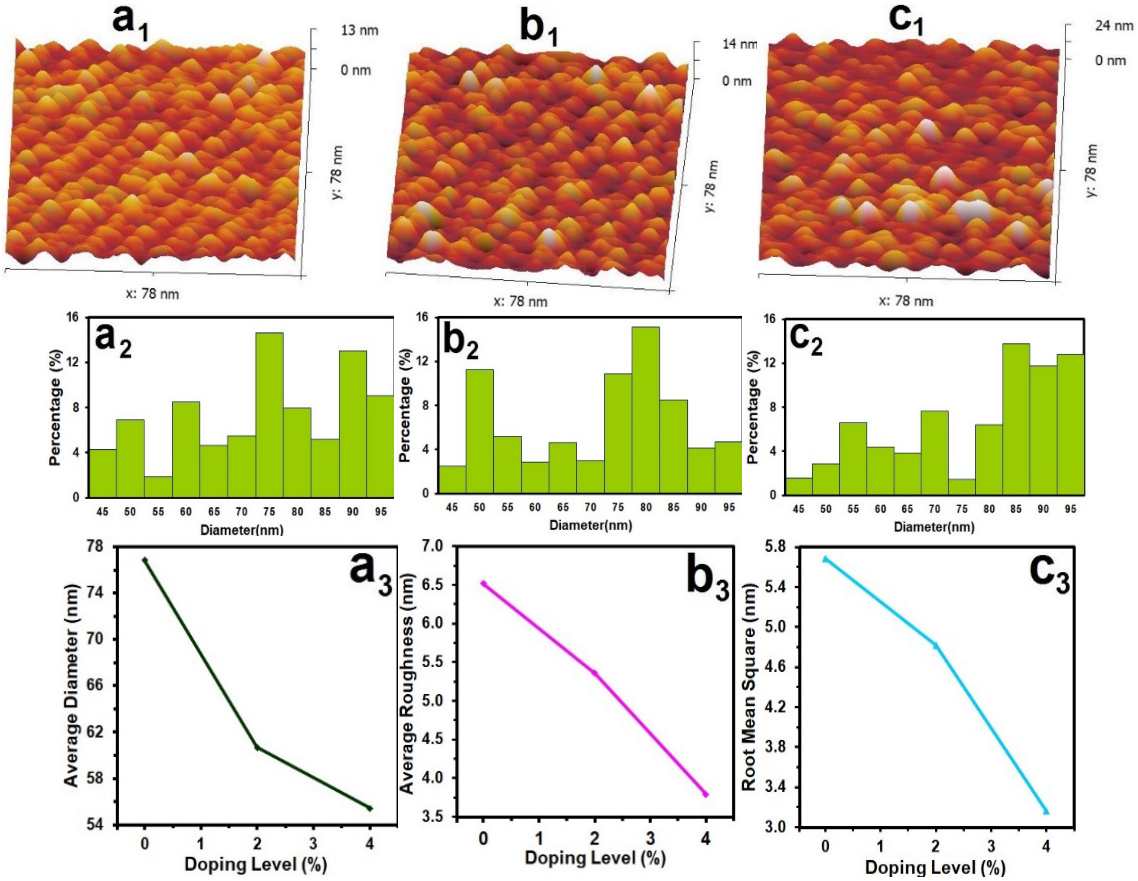

Fig. 3. AFM. of Undoped & TiO_2: Ag films.

Table 2. AFM parameter measurement of Undoped and TiO_2:Ag films.

Samples	**Average Particle size nm**	**R_a (nm)**	**R. M. S. (nm)**
Undoped TiO_2	76.82	6.52	5.68
TiO_2: 2% Ag	60.67	5.36	4.82
TiO_2: 4% Ag	55.43	3.79	3.16

The SEM pictures of the synthesised films from Undoped TiO_2, TiO_2: 2% Ag, TiO_2: 4% Ag are displayed in Fig. (4). The SEM images reveal a distinct transformation in the synthesized films. Initially characterized by flat islands, the surface undergoes a significant change, transitioning into uniformly covered spherical nano-grains following Ag doping. The observed decrease in the size of these nano-grains as Ag doping increases suggests a correlation between the doping concentration and the resulting nanostructure. This phenomenon is likely influenced by the interaction between the added silver (Ag) and the TiO_2 matrix, impacting the growth and arrangement of nanostructures during film synthesis [32].

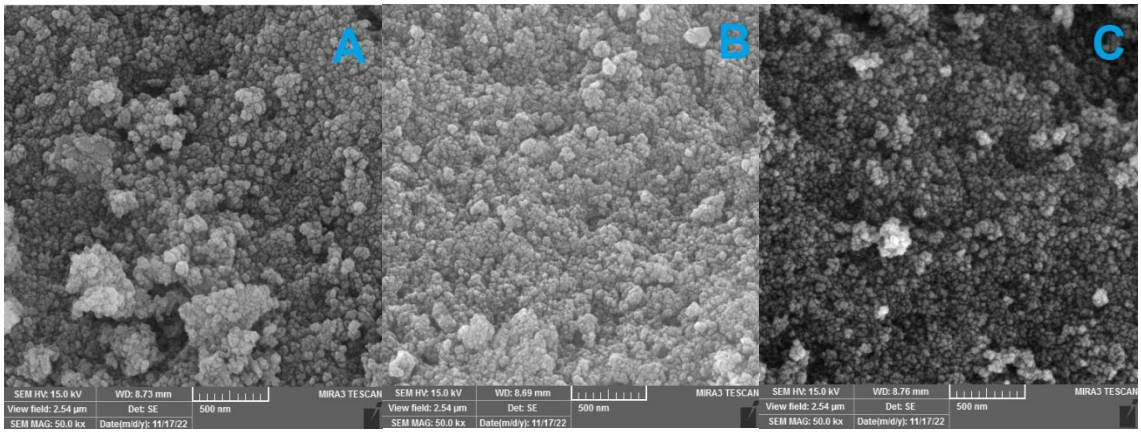

Fig. 4. SEM images of TiO_2: (a) Undoped, (b) 2% Ag, (c) 4% Ag.

The optical transmission (T) spectra of the intended films are shown in Fig. 5. T of Undoped TiO_2 is about 75 % in the visible area, and after doping it is increased to 65 %, which may be due to the grain boundary scattering [35].

The absorption coefficient (α) is illustrated in equation 4 [36]:

$$\alpha = 2.303\ (A/d) \tag{4}$$

where A is absorbance, and d is film thickness. The intended films are varied with Ag contents that are determined from absorbance measurements using equation (4) is shown in Fig. (6) A dropped abruptly at the UV/VIS boundary and progressively in visible areas [37]. As a result, Ag doping lowers the bandgap energy. The higher the Ag content, the greater the absorption of shorter wavelengths. A comparable study found that the absorption edge shift was presumably caused by silver and TiO_2 interaction [38].

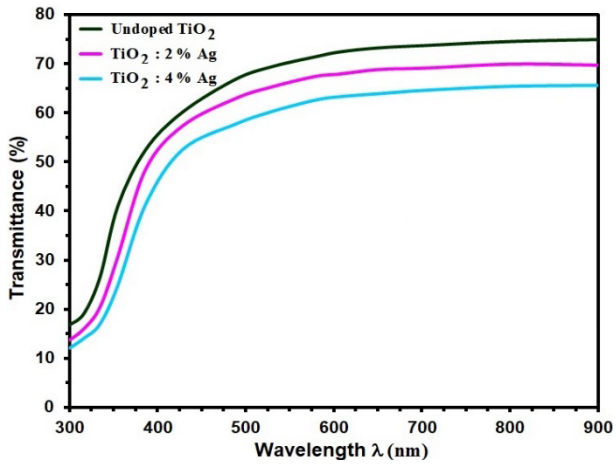

Fig. 5. Transmittance of Undoped and TiO_2:Ag films with different dopant.

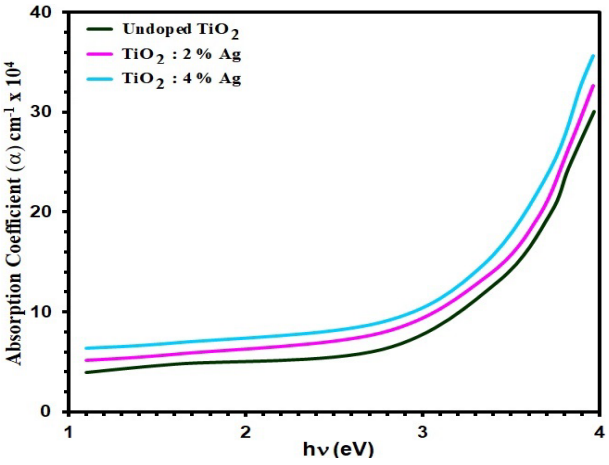

Fig. 6. α of Undoped and TiO_2:Ag films with different dopant.

The direct band transition is given by [39]:

$$(\alpha h\nu)^2 = B(h\nu - E_g) \tag{5}$$

where B is a constant, h ν is incident photon energy.

The graph of $(\alpha h\nu)^2$ vs hv of the intended films, which was used to determine bandgap, is depicted in Fig. (7). Because the linear part of $(hv)^2$ increases linearly with photon energy at increasing photon energies, it is concluded that the intended films feature direct band transitions.. The linear of the curve, when extrapolated to zero, gives the optical band gap value. The energy bandgap of the intended films decreased with Ag doping for all films, as seen in Fig. (6). Previous studies [29] have found similar results. Ag doping resulted in increased localized near valence and conduction bands. This can be assigned to the larger particle sizes or the increased size of particles. Ag doping reduced bandgap energy, preventing charge recombination between electron-hole pairs [40].

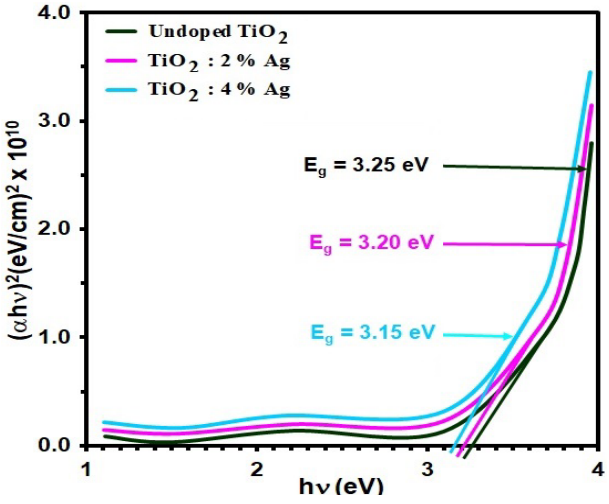

Fig. 7. direct band gap (E_g) of Undoped and TiO_2:Ag films with different dopants.

Fig. (8) Shows the diversity in extinction coefficient k of TiO_2 films with wavelength. The figure shows that k has the same behaviour refractive index. The influence of Ag content on k values is observed, showcasing a decrease in the extinction coefficient values with an increase in

doping concentration. This decrease is attributed to heightened absorption, contributing to a reduction in defects or deep tails, ultimately resulting in lower extinction coefficient values [41].

Since the dispersion energy depends on the optical transition and the optical conductivity, the refractive index (n) is a crucial element in fabricating devices with desirable optical properties. [42]. Fig. (9) Shows the diversity in refractive index (n) of TiO_2 films with wavelength.

Equation 6 was used to K of the intended films [43]:

$$k = \frac{\alpha\lambda}{4\pi} \tag{6}$$

Equation 7 was used to n of the intended films [44]:

$$n = \frac{1+R}{1-R}\sqrt{\frac{4R}{(1-R)^2} - k^2} \tag{7}$$

where R is the reflectance. n variation with λ of the intended films is shown in Fig. 8. n for both films reveals a similar trend. The curve drastically falls in the λ range of 400 to 600 nm and then gently increases with a further wavelength increase after a dramatic rise in the 400 to 600 nm [45].

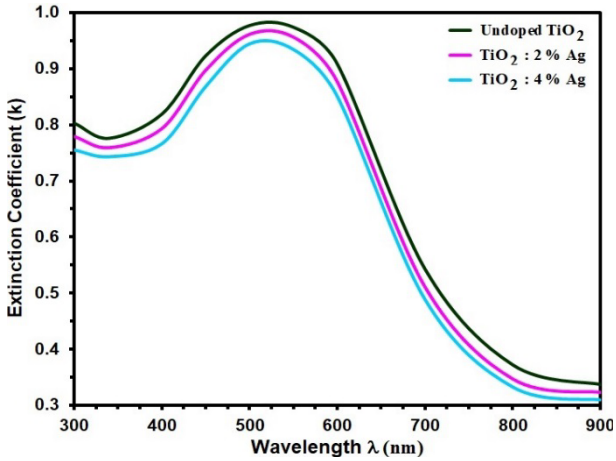

Fig. 8. k of Undoped and TiO_2:Ag films with different dopant.

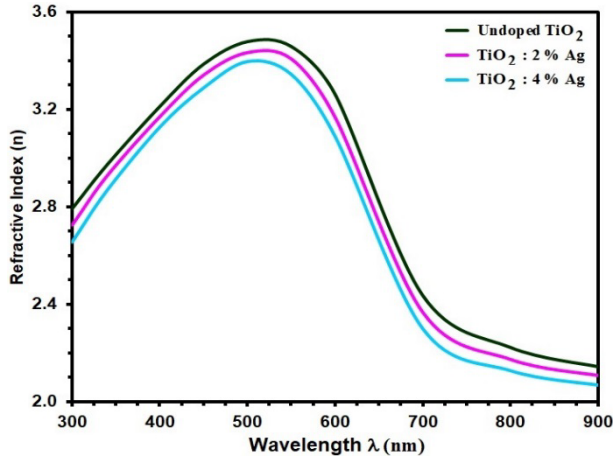

Fig. 9. n of Undoped and TiO_2: Ag films with different dopant.

The detection sensitivity, or response of the sensor, can be computed as [46]:

$$Sensitivity = \frac{\Delta R}{R_g} = \left|\frac{R_g - R_a}{R_g}\right| \times 100\ \% \tag{8}$$

The gas sensor, fabricated using porous silicon and avia TiO_2 thin film on glass, was tested against oxidizing gas (NH_3) at a concentration of 250 ppm. Figure (10) illustrates the relationship between resistance and time for Undoped, TiO_2: 2% Ag and TiO_2: 4% Ag at 250 ppm, operating at a temperature of 150 °C. The presence of NH_3 molecules leads to an oxidation process on the surface. As specific O^{2+} ions release bonded electrons to the surface, these electrons drift back to the conduction band [48], resulting in increased resistance and an enhanced potential barrier under these conditions [49]. Furthermore, it was observed that the TiO_2 film at 4% Ag doping exhibited the highest resistance.

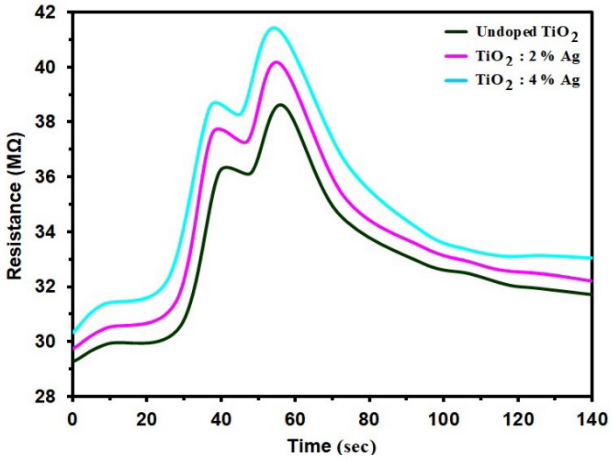

Fig. 10. Resistance as a function of operating time for Undoped and TiO_2: Ag films with different dopant.

The sensitivity plots in Figure (11) illustrate the impact of Undoped, TiO_2: 2% Ag and TiO_2: 4% Ag, on NH_3 gas exposure. The recombination process between charge carriers influences sensitivity, revealing a reduction with increasing Ag doping [50] . For varied Undoped, TiO_2: 2% Ag and TiO_2: 4% Ag, sensitivity decreased from 18.4 % to 4.6 % (50 ppm), 20.7 % to 6.8 % (150 ppm), and 25.9 % to 8.2 % (250 ppm) [51,52]. Sensitivity decreased for Undoped, TiO_2: 2% Ag, and TiO_2: 4% Ag, indicating that higher Ag doping levels led to a decline in the sensor's responsiveness to NH_3 gas.

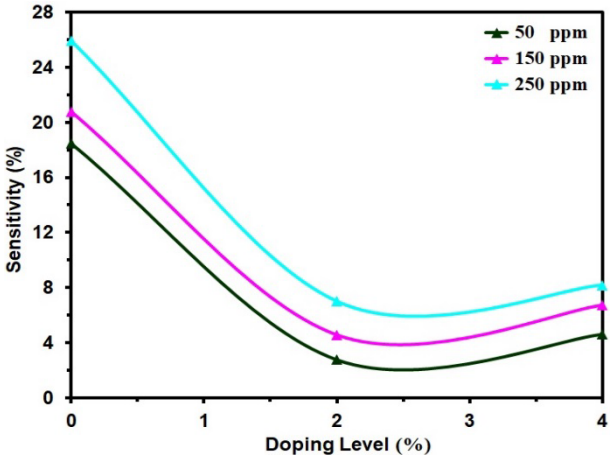

Fig. 11. Sensitivity of Undoped and TiO_2: Ag films with different dopant.

4. Conclusion

Undoped and Ag-doped TiO_2 thin films were prepared using the CSP method on a glass slide at 450ºC. XRD AFM and UV-VIS spectrophotometer techniques characterized all thin films. From XRD results, the rystallite size of TiO_2: Ag increased slightly compared with TiO_2. AFM studies estimated that the average particle size measurement of the TiO_2 surface is 76.82nm and decreases with Ag 3% doping to arrive at 55.43nm. SEM images depict the surfaces of TiO_2 films, revealing evident surface transformation characterized by uniform spherical nano-grains following Ag doping. The optical research showed that the energy gap of TiO_2 films has a substantial influence on the properties of the films, and it was discovered that the bandgap of TiO_2 can be vast and decrease with increasing doping. Increased Ag doping reduces E_g, n, and k values for all films (k). NH_3 gas sensor displayed heightened resistance at 250 ppm, suggesting sensitivity. TiO_2 at 4% Ag demonstrated the maximum resistance. Sensitivity decreases with higher Ag doping for NH_3 gas.

Acknowledgements

The authors express their gratitude to Mustansiriyah University (uomustansiriyah.edu.iq), research lab at the college of education, Garmian university and Alnukhba University College for their support in conducting this work.

References

[1] M. Al-Zahrani , N.S. Alsaiari, T. Radika , K. M. Abualnaja , R. Jothiramalingam , M. Ouladsmane, J. Ovonic Res., 18, 101-112 (2022); https://doi.org/10.15251/JOR.2022.181.101
[2] Y. Lin, Z. Jiang, C. Zhu, R. Zhang, X. Hu, X. Zhang, H. Zhu, S.H. Lin, Int. J. Hydrogen Energy, 42, 4966-4976 (2017); https://doi.org/10.1016/j.ijhydene.2016.06.077
[3] D. Zhu, L. Cai, Z. Sun, A. Zhang, P. Héroux, H. Kim, W. Yu, Y. Liu, Sci. Total Environ, 787, 147536 (2021); https://doi.org/10.1016/j.scitotenv.2021.147536
[4] N. N. Jandow, M. S. Othman, N. F.Habubi, S. S. Chiad, K. A. Mishjil, I. A. Al-Baidhany, Materials Research Express, 6 (11), (2020); https://doi.org/10.1088/2053-1591/ab4af8
[5] M. S. Othman, K. A. Mishjil, H. G. Rashid, S. S. Chiad, N. F. Habubi, I. A. Al-Baidhany, Journal of Materials Science: Materials in Electronics, 31(11), 9037-9043 (2020); https://doi.org/10.1007/s10854-020-03437-0
[6] A. J. Haider, R. Hassan AL-Anbari, G. Rasim Kadhim, and C. Touma Salame, *Energy Procedia,* 119, 332-345 (2017); https://doi.org/10.1016/j.egypro.2017.07.117
[735] E. S. Hassan, K. Y. Qader, E. H. Hadi, S. S. Chiad, N. F. Habubi, K. H. Abass, Nano Biomedicine and Engineering, 12(3), pp. 205-213 (2020); https://doi.org/10.5101/nbe.v12i3.p205-213
[7] E. H. Hadi, D. A. Sabur, S. S. Chiad, N. F. Habubi, K., Abass, Journal of Green Engineering, 10 (10), 8390-8400 (2020); https://doi.org/10.1063/5.0095169
[8] W. Kangwansupamonkon, N. Klaikaew, S. Kiatkamjornwong, Eur. Polym. J., 107, 118-131(2018); https://doi.org/10.1016/j.eurpolymj.2018.08.004
[9] Khadayeir, A. A., Hassan, E. S., Mubarak, T. H., Chiad, S.S., Habubi, N. F., Dawood, M.O., Al-Baidhany, I. A., Journal of Physics: Conference Series, 1294 (2) 022009(2019); https://doi.1088/1742-6596/1294/2/022009
[10] M. D. Sakhil, Z. M. Shaban, K. S. Sharba, N. F. Habub, K. H. Abass, S. S. Chiad, A. S. Alkelaby, NeuroQuantology, 18 (5), 56-61 (2020); https://doi.org/10.14704/nq.2020.18.5.NQ20168
[12] C.Yang, H. Fan, Y.e Xi, J. Chen, Z. Li, Applied Surface Science, 254, 2685–2689 (2008); https://doi.org/10.1016/j.apsusc.2007.10.006
[13] W. Yang, C. A. Wolden, Thin Solid Films, 515, 1708–1713 (2006);

https://doi.org/10.1016/j.tsf.2006.06.010
[14] A. Sharma, A. Gouldstone, S. Sampath, R. J. Gambino, J. Appl. Phys., 100, 114906 (2006); https://doi.org/10.1063/1.2382456
[15] S. S. Chiad, T. H. Mubarak, International Journal of Nanoelectronics and Materials, 13 (2), 221-232 (2020).
[16] N. Inoue, H. Yuasa, M. Okoshi, Applied Surface Science., 197 (198), 393–397 (2002); https://doi.org/10.1016/S0169-4332(02)00347-1
[17] B. Morris Henry, US Patent, 4, 474 (1978); https://doi.org/10.1147/rd.433.0383
[18] A. J. Kadhm, I. A. Abbas, Nano Biomedicine and Engineering, 14(4), 360–366 (2022); https://doi.org/10.5101/nbe.v14i4.p360-366
[19] A. A. Abdul Razaq , F. H. Jasim , S. S. Chiad , F. A. Jasim, Z. S. A. Mosa , Y. H. Kadhimd, Journal of Ovonic Research, 20 (2), 131 – 141 (2024); https://doi.org/10.15251/JOR.2024.202.131
[20] Cheol Ho Heo, Soon-Bo Lee, Jin-Hyo Boo, Thin Solid Films, 475, 183– 188 (2005); https://doi.org/10.1016/j.tsf.2004.08.033
[21] S. K. Muhammad, E. S. Hassan, K. Y. Qader, K. H. Abass, S. S. Chiad, N. F. Habubi, Nano Biomedicine and Engineering, 12 (1), 67-74 (2020);
https://doi.org/10.5101/nbe.v12i1.p67-74
[22] K. H. Jebur, N. J. Mohammed, Al-Mustansiriyah Journal of Science, 32(4), 60-66 (2021);
http://doi.org/10.23851/mjs.v32i4.993
[23] S. A. Hasan, J. A. Salman, S. S. Al-Jubori, Al-Mustansiriyah Journal of Science, 32(4), 21-25 (2021); http://doi.org/10.23851/mjs.v32i4.1034
[24] A. A. Z. Alaabedin, B. H. Hamza, A. Mu. Abdual-Majeed, S. F. Bamsaoud, Al-Mustansiriyah Journal of Science, 34 (3), 115-123 (2023); https://doi.org/10.23851/mjs.v34i3.1339
[25] T. Huang, W. Huang, C. Zhou, Y. Situ, H. Huang, *Surface and Coatings Technology* 213, (2012); https://doi.org/10.1016/j.surfcoat.2012.10.033
[26] A. J. Ghazai, O. M. Abdulmunem, K. Y. Qader, S. S. Chiad, N. F. Habubi, AIP Conference Proceedings 2213 (1), 020101 (2020); https://doi.org/10.1063/5.0000158
[27] N. Y. Ahmed, B. A. Bader, M. Y. Slewa, N. F. Habubi, S. S. Chiad, NeuroQuantology, 18(6), 55-60 (2020); https://doi.org/10.1016/j.jlumin.2021.118221
[28] N. N. Jandow, N. F. Habubi, S. S. chiad, I. A. Al-Baidhany and M. A. Qaeed, International Journal of Nanoelectronics and Materials, 12 (1), 1-10 2019.
[29] S. S. Chiad, H. A. Noor, O. M. Abdulmunem, N. F. Habubi, M. Jadan, J. S. Addasi, Journal of Ovonic Research, 16 (1), 35-40 (2020).
[30] M. Yazıcıa, O. Çomaklı, T. Yetim, A. F. Yetim, A. Çelik, *Tribology International,* 104, 175-182 (2016); https://doi.org/10.1016/j.triboint.2016.08.041
[31] H. T. Salloom, E. H. Hadi, N. F. Habubi, S. S. Chiad, M. Jadan, J. S. Addasi, Digest Journal of Nanomaterials and Biostructures, 15 (4), 189-1195 (2020);
https://doi.org/10.15251/DJNB.2020.154.1189
[32] H. A. Hussin, R. S. Al-Hasnawy, R. I. Jasim, N. F. Habubi, S. S. Chiad, Journal of Green Engineering, 10(9), 7018-7028 (2020); https://doi.org/10.1088/1742-6596/1999/1/012063
[33] S. S Chiad,, A. S. Alkelaby, K. S. Sharba,, Journal of Global Pharma Technology, 11 (7), 662-665, (2020); https://doi.org/10.1021/acscatal.1c01666
[34] R. S Ali, N. A. H. Al Aaraji, E. H. Hadi, N. F. Habubi, S. S. Chiad, Journal of Nanostructuresthis link is disabled, 10(4), 810–816 (2020); https://doi: 10.22052/jns.2020.04.014
[35] A. A. Khadayeir, R. I. Jasim, S. H. Jumaah, N. F, Habubi, S. S. Chiad, Journal of Physics: Conference Series,1664 (1) (2020); https://doi.org/10.1088/1742-6596/1664/1/012009
[36] Chiad, S.S., Noor, H.A., Abdulmunem, O.M., Habubi, N.F., Journal of Physics: Conference Series 1362(1), 012115 (2019); https://doi.org/10.1088/1742-6596/1362/1/012115
[37] A. S. Al Rawas, M. Y. Slewa, B. A. Bader, N. F. Habubi, S. S. Chiad, Journal of Green Engineering,10 (9), 7141-7153 (2020); https://doi.org/10.1021/acsami.1c00304
[38] S. S. Chiad, N. F. Habubi, W. H. Abass, M.H. Abdul-Allah, Journal of Optoelectronics and Advanced Materials, 18(9-10), 822-826, (2016).

[39] M. I. Kanjal, M. Muneer, M. Saeed, W. Chu, N. Alwadai, M. Iqbal, A. Abdelhaleem, Ara. J. Chem. 15(9), 104061 (2022); https://doi.org/10.1016/j.arabjc.2022.104061
[40] R. S. Ali, M. K. Mohammed, A. A. Khadayeir, Z. M. Abood, N. F. Habubi and S. S. Chiad, Journal of Physics: Conference Series, 1664 (1), 012016 (2020); https://doi:10.1088/1742-6596/1664/1/012016
[40] K. Y. Qader, R. . Ghazi, A. M. Jabbar, K. H. Abass, S. S. Chiad, Journal of Green Engineering, 10 (10), 7387-7398, 2020. https://doi.org/10.1016/j.jece.2020.104011
[41] Hassan, E.S., Mubarak, T.H., Chiad, S.S., Habubi, N.F., Khadayeir, A.A., Dawood, M.O., Al-Baidhany, I. A. , Journal of Physics: Conference Series, 1294(2), 022008 (2019); https://doi.1088/1742-6596/1294/2/022008
[42] R. S. Ali, H. S. Rasheed, N. F. Habubi, S.S. Chiad, Lettersthis link is disabled, 20(1), 63–72 (2023; https://doi.org/10.15251/CL.2023.201.6
[43] R. Kumar, A. K. Singh, P. S. Mondal, Materials Today: Proceedings, 66(7), 3244–3249 (2022); https://doi.org/10.1016/j.matpr.2022.06.257
[44] Y. Mingmongkol, D. T. T. Trinh, P. Phuinthiang, D. Channei, K. Ratananikom, A. Nakaruk, W. Khanitchaidecha, Nanomaterials, 12, 1198 (2022); https://doi.org/10.3390/nano12071198
[45] A. Ghazai, K. Qader, N. F. Hbubi, S. S. Chiad, O. Abdulmunem, IOP Conference Series: Materials Science and Engineering, 870 (1), 012027 (2020); https://doi.org/ 10.1088/1757-899X/870/1/012027
[46] B. A. Bader, S. K. Muhammad, A. M. Jabbar, K. H. Abass, S. S. Chiad, N. F. Habubi, J. Nanostruct 10(4): 744-750 (2020); https://doi.org/ 10.22052/JNS.2020.04.007
[47] E. H. Hadi, M. A. Abbsa, A. A. Khadayeir, Z. M. Abood, N. F. Habubi, and S.S. Chiad, Journal of Physics: Conference Series, 1664 (1), 012069 (2020); https://doi.org/ 10.1088/1742-6596/1664/1/012069
[48] O. M. Abdulmunem, A. M. Jabbar, S. K. Muhammad, M. O. Dawood, S. S. Chiad, N. F. Habubi, Journal of Physics: Conference Series,1660 (1), 012055 (2020); https://doi.org/ 10.1088/1742-6596/1660/1/012055
[49] S. Muthukrishnan, R. Vidya, A. O. Sjåstad, Mater. Chem. Phys. 299, 127467 (2023); https://doi.org/10.1016/j.matchemphys.2023.127467
[50] M.O. Dawood, S.S. Chiad, A.J. Ghazai, N.F. Habubi, O.M. Abdulmunem, AIP Conference Proceedings 2213, 020102,(2020); https://doi.org/10.1063/5.0000136
[51] B. Zhang, H. Wang, J. Luo, S. Liu, Y. Tian, J. Electroanal. Chem. 930, 117159 (2023); https://doi.org/10.1016/j.jelechem.2023.117159
[52] A. A. Khadayeir, E. S. Hassan, S. S. Chiad, N. F. Habubi, K. H. Abass, M. H. Rahid, T. H. Mubarak, M. O. Dawod, and I.A. Al-Baidhany, Journal of Physics: Conference Series 1234 (1), 012014, (2019); https://doi.1088/1742-6596/1234/1/012014